

## USING ULTRASONIC DOPPLER VELOCIMETRY AND CFD MODELING TO INVESTIGATE THE MIXING OF NON-NEWTONIAN FLUIDS POSSESSING YIELD STRESS

F. Ein-Mozaffari, S. R. Upreti

*Department of Chemical Engineering, Ryerson University, 350 Victoria Street  
Toronto, Ontario, M5B 2K3, Canada; Email: [fmozaffa@ryerson.ca](mailto:fmozaffa@ryerson.ca)*

**Abstract.** The aim of this work was to investigate the mixing of pseudoplastic fluids possessing yield stress by studying the effect of power consumption, yield stress, impeller type, and impeller clearance on the mixing time. Using these results, it was desired to put together a proposal for mixing system configuration that would form the basis for mixing system optimization. To that end, computational fluid dynamics (CFD) modeling and experiments were performed. In order to determine the capability of CFD to forecast the mixing process, ultrasonic Doppler velocimetry (UDV), which is a non-invasive flow measurement technique for both opaque and transparent fluids, was used to measure fluid velocity. It was observed that the numerical results were in good agreement with the experimental data.

**Key words:** Mixing of Non-Newtonian Fluids; Computational Fluid Dynamics; Ultrasonic Doppler Velocimetry; Yield Stress; Mixing Time; Pseudoplastic Fluids.

### 1. INTRODUCTION

Mixing is a common unit operation in the chemical and process industries and frequently involves non-Newtonian fluids. Majority of these non-Newtonian fluids are pseudoplastic. Some also possess a yield stress which means that the fluid will not flow unless the applied stress exceeds the yield stress value. For such pseudoplastic fluids possessing a yield stress, there is usually the formation a zone of intense motion (cavern) in the impeller region surrounded by stagnant and/or slow-moving fluids in the mixing vessel [1]. These poor mixing conditions have been implicated in product degradation, poor heat transfer rates, and loss in productivity. The mixing performance of impellers can be assessed by the measurement of a key performance indicator known as the mixing time. Mixing time provides a measure of homogeneity of the mixing system and is mainly useful for comparing different agitator systems. Therefore, the measurement of mixing time is crucial to the evaluation of mixing system efficiency. The mixing time can be obtained via physical experiments or through computational fluid dynamics (CFD).

Several experimental techniques have been employed to measure the mixing time, such as dye addition, conductivity probe, laser-induced fluorescence, liquid-crystal thermography, radioactive liquid tracer, and tomography techniques [2]. Some of these methods are not applicable for the opaque fluids and the probe techniques have the disadvantage of affecting the flow pattern inside the tank. The advantage of CFD over these experimental techniques is that it provides comprehensive data that are not easily obtained from experimental tests. A few publications have been devoted to the simulation of mixing time for non-Newtonian fluids using CFD modeling [3-6]. From the literature review, it is clear that the mixing performance of impellers in highly viscous shear thinning fluids possessing a yield stress needs to be investigated as little research has been devoted to the numerical simulation of homogenization in stirred tanks containing non-Newtonian fluids. A study of the effect of mixing system configuration, fluid

properties, and power consumption on the mixing time represents necessary steps towards optimization of the mixing system. Therefore, the aim of this work is to use CFD as a tool to study and assess the performance of three different impellers in mixing of pseudoplastic fluids possessing yield stress. The velocity profiles measured using the ultrasonic Doppler velocimetry are used to validate the CFD model.

## 2. EXPERIMENTAL SETUP AND PROCEDURES

The experimental setup (Figure 1) used in this work consists of a transparent cylindrical tank of diameter ( $T$ ) 20 cm. The flat-bottomed tank was fitted with four equally spaced flat baffles each with a width ( $w$ ) equal to 10% of the tank diameter. The fluid height ( $H$ ) was maintained constant at a height equal to the tank diameter. Three axial flow impellers were utilized in the experiments: pitched blade turbine (PBT), marine propeller, and A310 impeller, each having a diameter ( $D$ ) equal to  $0.44T$ . The impellers were mounted on a centrally located shaft and driven by a variable-speed motor. The impeller clearance was varied from  $H/3$  to  $H/2$ . Impeller torque and speed were measured using a rotary torque transducer with an encoder disk (Staiger Mohilo, Germany).

The test fluids employed for all the experiments were aqueous solutions of xanthan gum with concentrations ranging from 0.5 wt % to 1.5 wt %. Aqueous solutions of xanthan gum are pseudoplastic and possess a yield stress. The rheology of the test solutions was measured using a Bohlin Rheometer (Malvern Instruments Ltd., UK). The resulting rheological data were fitted to the Herschel-Bulkley rheological model [7]:

$$\tau = \tau_y + K \dot{\gamma}^n \quad (1)$$

where  $\tau$ ,  $\tau_y$ ,  $K$ ,  $\dot{\gamma}$  and  $n$  are the shear stress, yield stress, consistency index, shear rate, and flow behavior index, respectively, with values for the xanthan gum solutions shown in Table 1. The density ( $\rho$ ) of the solutions was measured using a pycnometer.

**Table 1.** Rheological properties of xanthan gum solutions

| Concentration<br>(wt %) | $\tau_y$<br>[Pa] | $K$<br>[Pa.s <sup>n</sup> ] | $n$<br>[-] | $\rho$<br>[kg/m <sup>3</sup> ] |
|-------------------------|------------------|-----------------------------|------------|--------------------------------|
| 0.5                     | 1.79             | 3                           | 0.11       | 997                            |
| 1.0                     | 5.25             | 8                           | 0.12       | 992                            |
| 1.5                     | 7.45             | 14                          | 0.14       | 990                            |

An ultrasound Doppler velocimeter (UDV) was employed to measure velocity profiles within the vessel. UDV (Signal Processing, Switzerland) utilizes a pulsed ultrasonic echography together with the detection of the instantaneous frequency of the detected echo which gives the spatial information and estimates of the Doppler shift frequency, respectively. It is from the Doppler shift frequency that the magnitude and direction of the velocity vector is obtained [8]. UDV method is a non-invasive method of measuring velocity profiles and can therefore be used to monitor the flow in stirred tanks without obstructing it. The ability to work in opaque fluids makes UDV applicable for studies of all liquids, emulsions, and slurries and makes this technique very attractive from an industrial perspective [5]. Generally, an ultrasonic pulse is emitted into the medium along the measuring line by a piezoelectric transducer ultrasonically coupled to the outside of the vessel. This transducer receives the echo reflected from the surface

of microparticles suspended in the medium. The detected echo contains the velocity profile information. The position ( $I$ ) of the particle (from which the echo is reflected) along the probe axis is determined from the time delay ( $T_d$ ) between pulse emission and echo reception [5, 6, 8]:

$$\Gamma = \frac{v_s T_d}{2} \quad (2)$$

where  $v_s$  is the speed of sound in the fluid. The velocity of the particle ( $v$ ) is calculated from the Doppler shift frequency ( $F_d$ ), which is defined as the difference between the emitted and received frequency, and is given by [5, 6, 8]:

$$v = \frac{v_s F_d}{2 F_e \cos \theta} \quad (3)$$

where  $F_e$  is the emission frequency from the transducer and  $\theta$  is the Doppler angle (the angle the particle trajectory makes with the propagation direction of the ultrasonic wave). Figure 1 shows the locations of the UDV probes employed to measure the fluid time-averaged velocities inside the mixing vessel. Probe #1 was installed on the fluid surface ( $H_1 = z/H = 0.95$ ) and between two adjacent baffles at  $R_1 = r/(T/2) = 0.70$  to measure the velocity profile along the tank wall. Probe #2 was attached to the outside wall and between two adjacent baffles at  $H_2 = z/H = 0.25$  to measure the velocity profiles in front of the impeller. Since the ultrasonic signals can pass through the vessel wall, no special window on vessel wall was required. The UDV spatial resolution was about 2 mm.

### 3. CFD SIMULATIONS

CFD simulations were conducted using the commercial software package, Fluent 6.3. The conservation of mass and momentum equations were solved using the finite volume method. The first step in this method is to divide the spatial domain into small cells. The tetrahedral cells were used to generate the unstructured grid for the simulation. To verify the grid independency, the number of cells was increased by a factor of about 2. Grid independence was confirmed by demonstrating that additional cells did not change the calculated velocity magnitude measured in the regions of high velocity gradients

close to the impeller blades by more than 5%. The original 3D mesh of the model for pitched blade turbine had 103,323 cells. To verify the grid independency, their number increased to 205,098. This increase changed the velocity in regions of high velocity gradients by more than 5%. When the number of cells was further increased to 413,721, the velocity in the regions of high velocity gradients did not change by more than 5%. Therefore, 205,098 cells were employed for pitched blade impeller. The same approach was used to determine the optimum number of cells for the other two impellers. The number of cells were 211,365 and 208,742 for the marine propeller and A310, respectively. To realistically model the rotation of the impeller in the mixing vessel, the steady state multiple reference frames (MRF) technique was utilized. This technique has been found to yield flow field predictions comparable to those obtained using the time dependent sliding mesh (SM) impeller model [9]. Therefore, the MRF model is usually

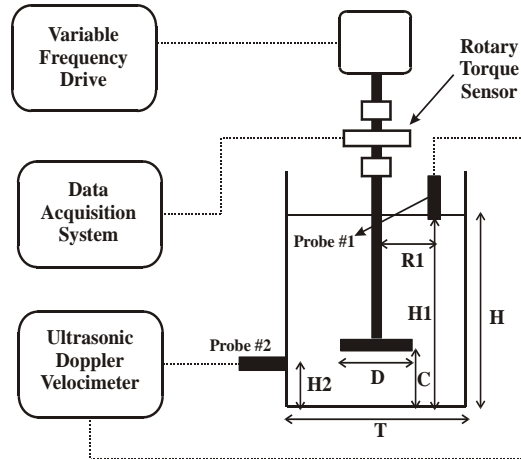


Figure 1: Experimental setup.

employed to reduce computational requirements. Computations were carried out using a 3.0 GHz Pentium 4 CPU with 2.0 GB RAM, and convergence was typically achieved after 5-6 h.

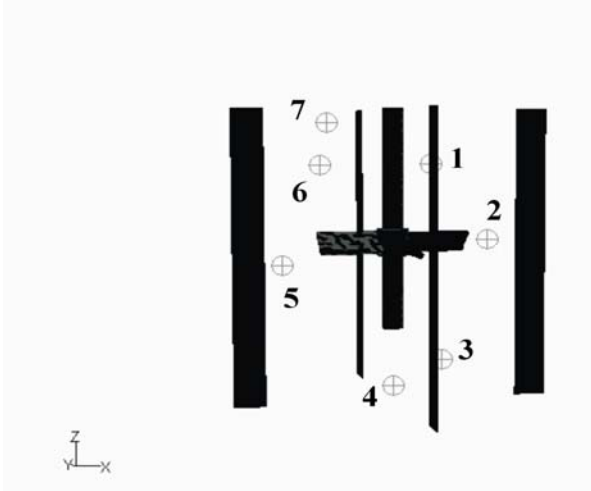


Figure 2: Monitoring points used to monitor the time evolution of tracer concentration.

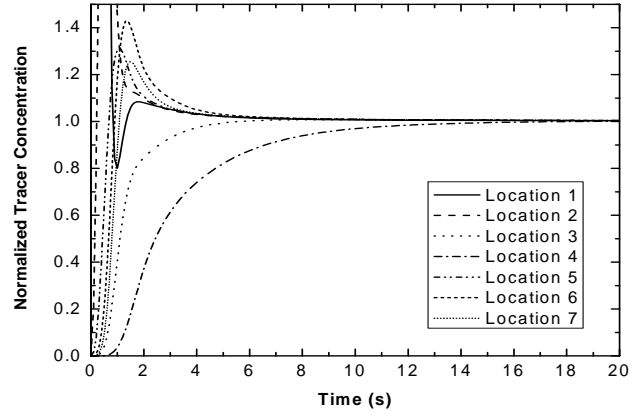


Figure 3: Normalized tracer concentration as a function of time at the monitoring points for 0.5% xanthan gum agitated with the PBT impeller at  $N = 210$  rpm (clearance =  $H/2$ ).

To simulate the mixing times after the convergence of the flow field, the unsteady state transport of an inert tracer superimposed on the calculated flow field was monitored until complete homogenization was achieved. The unsteady distribution of the tracer was determined by solving the species transport equation, based on the assumption that the tracer is distributed by convection and diffusion:

$$\frac{\partial}{\partial t}(\rho m_i) + \text{div}(\rho v m_i) = \text{div}(\Gamma_i \cdot \text{grad}(m_i)) \quad (4)$$

where  $m_i$  is the mass fraction of the tracer species,  $v$  is the mean velocity vector and  $\Gamma_i$  is the molecular diffusivity. The value of the molecular diffusivity used in this work was  $10^{-9}$  m<sup>2</sup>/s, a typical value for liquids even though this value was found to have a negligible effect on the tracer distribution possibly because the contribution of molecular diffusion to the overall tracer dispersion process is negligible [3]. A time step of 0.1 s was adopted for the mixing time simulations. The tracer addition point was at location 1 (Figure 2). The time evolution of tracer concentration was measured at 7 different locations including addition point. The mixing time was obtained by combining the normalized tracer distribution (normalized with the tracer concentration at steady state) at each of the monitoring points on a single graph, and taken to be the time when the normalized tracer concentration at each of the monitoring locations simultaneously reached within 98% of the steady state value (Figure 3). Mixing time was computed using both MRF and SM techniques and the variation was less than 5%. For instance, the mixing times calculated using MRF and SM methods at  $N = 400$  rpm and 1.5% xanthan gum were 92.5 s and 88.1 s, respectively. However, the computational time required for SM method was much higher ( $\approx 25$  h) than that for MRF technique ( $\approx 6$  h). Thus, MRF method was employed in this study to simulate the impeller rotation. Pakzad [10] also investigated the ability of the MRF method to predict the mixing time for the pseudoplastic fluids possessing yield stress agitated with a radial-flow impeller in a tank equipped with four baffles. She showed that the mixing times computed using MRF method were in good agreement with those measured using electrical resistance tomography.

#### 4. RESULTS AND DISCUSSION

To validate the model, CFD results for the power number and velocity field were compared to experimental data. Figure 4 shows the power number ( $P_o = P/\rho N^3 D^5$ , where  $P$ ,  $N$ ,  $D$ , and  $\rho$  are power, impeller speed, impeller diameter, and fluid density, respectively.) versus Reynolds number ( $Re$ ) for three impellers used in this study. Metzner-Otto correlation was used to obtain the Reynolds number for Herschel-Bulkley fluids [7]:

$$Re = \frac{\rho N^2 D^2 k_s}{\tau_y + K(k_s N)^n} \quad (5)$$

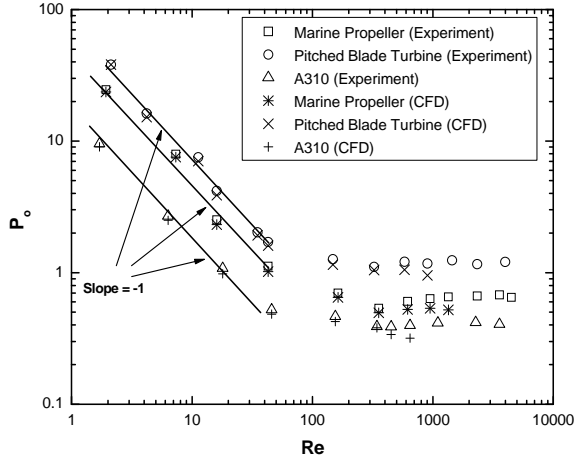


Figure 4: Power number versus Reynolds number.

These results show a good agreement between calculated power number and the experimentally determined values. There is a slight deviation at  $Re > 600$  which may be due to the use of the laminar flow model in transitional flow regime. The use of the laminar flow model in the transitional regime is quite common in numerical modeling as may be seen from the work of other researchers [11]. At low  $Re$  (in the laminar regime), power number is inversely proportional to Reynolds number ( $P_o \propto Re^{-1}$ ). CFD results for the velocity field were also compared to experimental data. Figure 5 shows a comparison of the velocity data from the UDV measurements with the velocities computed using CFD. It is observed that the CFD calculations pick up the features of the flow field, and the computed velocities agree well with the measured data.

Flow number can be estimated for axial flow impellers from the following equation using impeller pumping flow rate,  $Q_P$  [12]:

$$Fl = Q_P / ND^3 = 2\pi \int_0^{D/2} r v_z dr / (ND^3) \quad (6)$$

where  $r$  is radial coordinates and  $v_z$  is axial velocity. The axial velocities obtained using CFD and UDV were used to calculate the flow numbers for pitched blade turbine, marine propeller, and A310 impellers (Table 2). The number of data points considered for the calculation of the experimental and the simulated flow numbers were about 65 and 170, respectively. The average deviation was about 6%. It must be mentioned that the flow numbers calculated for xanthan gum solution in this study are less than those reported in literature for water. Other researchers have reported that the impeller flow number is a function of the rheological properties of the fluid (e.g. viscosity and yield stress) [8].

**Table 2:** Impeller flow numbers.

|                   | Marine Propeller | Pitched Blade Turbine | A310 |
|-------------------|------------------|-----------------------|------|
| Flow number (CFD) | 0.42             | 0.47                  | 0.37 |
| Flow number (UDV) | 0.39             | 0.43                  | 0.38 |

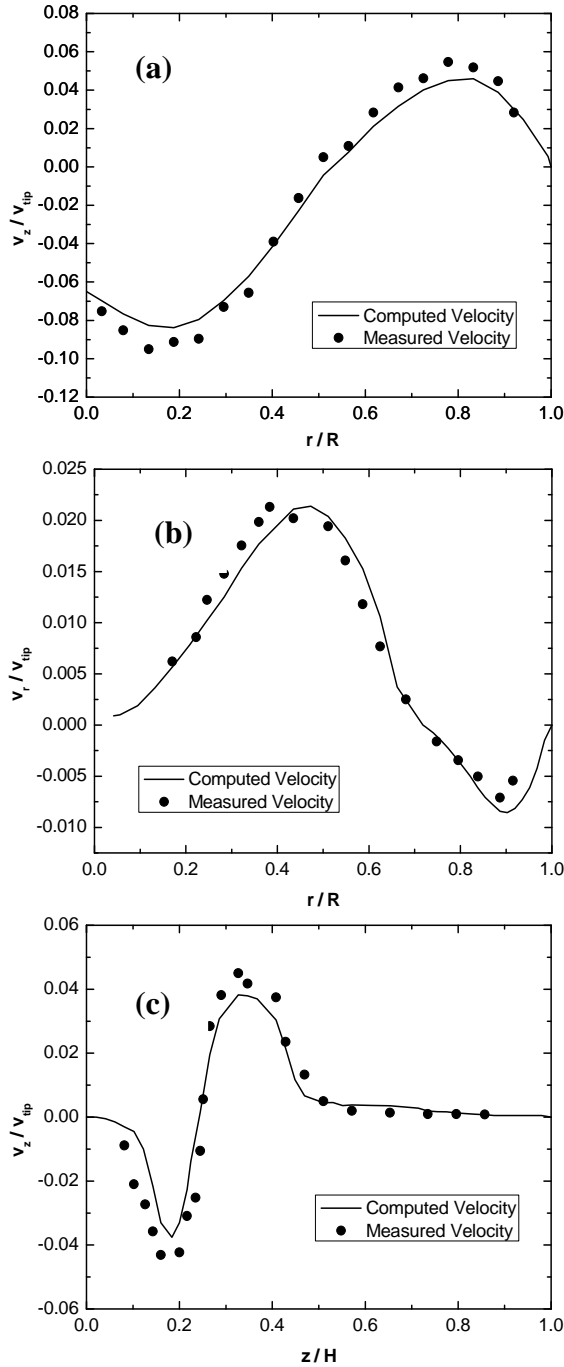


Figure 5: Computed and measured velocities for PBT impeller at  $Re = 72$  (a) axial velocity measured using Probe #2, (b) radial velocity measured using probe #2 and (c) axial velocity measured using probe #1.

where it was observed that increasing clearance gave lower mixing times. From Figure 8, it can be seen that for a given power input, the A310 impeller achieved homogenization in the shortest time. The results also show that the pitched blade turbine gives longer mixing times compared to the marine propeller, and A310 impeller at a specific power input.

Figure 6 shows the effect of xanthan gum concentration on the mixing time. For a given power input, as the concentration of xanthan gum was increased, the fluid yield stress increased causing an increase in the mixing time. A plausible explanation for this observation is that as the yield stress of the solutions increases for a given power input, low velocity conditions exist in a larger portion of the fluid in the tank resulting in an increase in the time required reaching homogeneity. In their investigation of mixing of pulp suspension, which possesses yield stress, Ein-Mozaffari et al. [13] showed that the fluid yield stress has a significant effect on the mixing time.

The effect of impeller clearance from the vessel bottom was studied using the pitched blade turbine impeller for the clearances ranging from  $H/3$  to  $H/2$ . The decision to study this range of clearance was made based on the knowledge that placing the impeller too low results in most of the fluid remaining unmixed, while operating at impeller clearances higher than half of the fluid height causes surface aeration even at low impeller rotational speeds. Figure 7 shows that as the clearance of the impeller was increased from  $H/3$  to  $H/2$ , the mixing time decreased. This result is identical to that obtained by Houcine *et al.* [14], who observed a reduction in the mixing time with increasing impeller clearance for the pitched blade turbine in the mixing of Newtonian fluids under turbulent conditions.

A comparison of mixing performance of the pitched blade turbine, marine propeller, and A310 impellers is made on the basis of equal power consumption. In order to accomplish this, the clearance of the impeller from the bottom of the tank was kept constant at  $H/2$ . The decision to study the mixing performance of the three impellers at this clearance was made based on the results obtained from the previous section

The ratio of the impeller flow number to power number, which is called pumping efficiency, has been frequently used in the literature to define the impeller efficiency [15]:

$$\eta_p = Fl / P_o \quad (7)$$

where  $\eta_p$ ,  $Fl$ , and  $P_o$  are pumping efficiency, impeller flow number, and power number, respectively. The power number and pumping efficiency of the three axial impellers tested in this study are listed in Table 3. This table shows that A310 and pitched blade turbine have the highest and the lowest pumping efficiency, respectively. As mentioned in previous section (see Figure 8), the pitched blade turbine was the least effective, while A310 was the most effective in reducing the mixing time. Thus, in order to minimize the mixing time, an impeller with a large pumping efficiency such as A310 should be chosen.

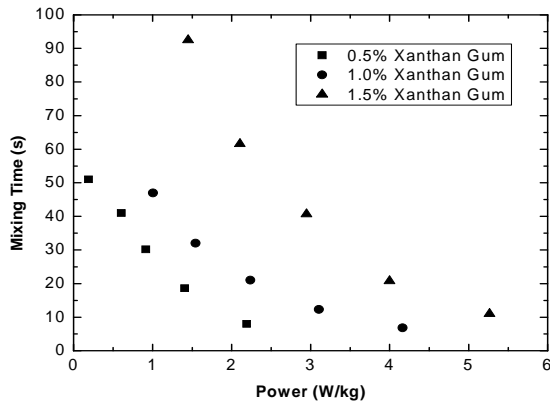


Figure 6: The effect of xanthan gum concentration on the mixing time for PBT impeller (clearance =  $H/2$ ).

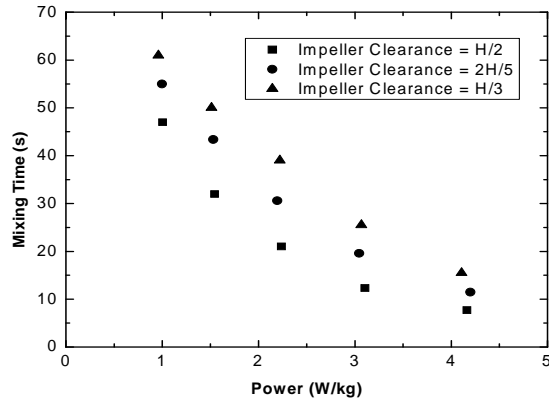


Figure 7: The effect of impeller clearance on the mixing time for 1.0% xanthan gum agitated by PBT impeller.

**Table 3: Impeller pumping efficiencies.**

|                    | Pitched Blade Turbine | Marine Propeller | A310 |
|--------------------|-----------------------|------------------|------|
| Power Number       | 1.16                  | 0.66             | 0.40 |
| Pumping Efficiency | 0.37                  | 0.59             | 0.95 |

## 5. CONCLUSIONS

The 3D flow field generated by the impeller in the agitation of xanthan gum solution was simulated using a CFD package. The rheology of the xanthan gum solution was approximated using Herschel-Bulkley model that contains a shear-thinning parameter and a yield stress. In order to validate the CFD model, the velocity profiles measured using ultrasonic Doppler velocimetry were compared to those computed using the CFD model. To simulate the mixing time, after the flow field had been calculated, the unsteady state transport of passive tracer superimposed on the calculated flow field was monitored until complete homogenization was achieved. The results showed that the fluid yield stress has a significant effect on the mixing time. It was observed that the mixing time decreased as the clearance of the impeller increased from  $H/3$  to  $H/2$ . The mixing performances of three impellers (pitched blade turbine, marine impeller, and A310 impeller) were evaluated on the basis of equal power consumption, and impeller pumping efficiency. It was found that an impeller with a larger pumping efficiency should be employed in order to reduce the mixing time.

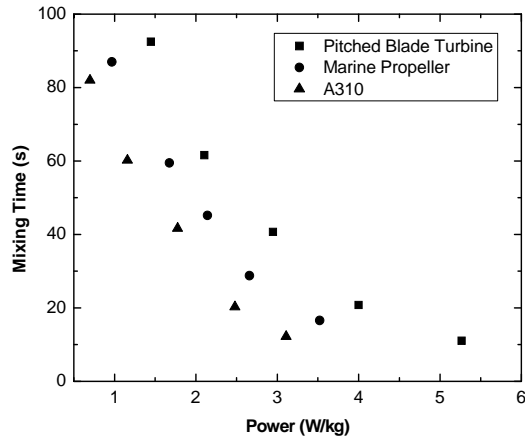


Figure 8: The effect of impeller type on the mixing time at 1.5% xanthan gum (clearance =  $H/2$ ).

## 6. REFERENCES

- Galindo E., Nienow A. W., 1992. "Mixing of highly viscous simulated xanthan fermentation broths with the Lightnin A-315 impeller", *Biotechnol. Prog.*, 8, 223-239.
- Paul E. L., Atiemo-Obeng V., Kresta S. M., 2004. *Handbook of industrial mixing: science & practice*. Wiley-Interscience, USA.
- Montante G., Mostek M., Jahoda M., Magelli F., 2005. "CFD simulations and experimental validation of homogenization curves and mixing time in stirred Newtonian and pseudoplastic liquids", *Chem. Eng. Sci.*, 60, 2427-2437.
- Rivera C., Foucault S., Heniche M., 2006. "Mixing analysis in a coaxial mixer", *Chem. Eng. Sci.*, 61, 2895-2907.
- Saeed S., Ein-Mozaffari F., Upreti S., 2007. "Using computational fluid dynamics modeling and ultrasonic Doppler velocimetry to study pulp suspension mixing", *Ind. Eng. Chem. Res.*, 46, 2172-2179.
- Ihejirika I., Ein-Mozaffari F., 2007. "Using CFD and ultrasonic velocimetry to study the mixing of pseudoplastic fluids with a helical ribbon impeller", *Chem. Eng. Technol.*, 30, 606-614.
- Pakzad L., Ein-Mozaffari F., Chan P., 2008. "Using electrical resistance tomography and computational fluid dynamics modeling to study the formation of cavern in the mixing of pseudoplastic fluids possessing yield stress", *Chem. Eng. Sci.*, 63, 2508-2522.
- Ein-Mozaffari F., Bennington C.P.J., Dumont G.A., Buckingham D., 2007. "Measuring flow velocity in pulp suspension mixing using ultrasonic Doppler velocimetry", *Chem. Eng. Res. Des.*, 85, 591-597.
- Brucato A., Ciofalo M., Crisfi F., Micale G., 1998. "Numerical prediction of flow fields in baffled stirred vessels: A comparison of alternative modeling approaches", *Chem. Eng. Sci.*, 53, 3653-3684.
- Pakzad, L., "Using Electrical Resistance Tomography and Computational Fluid Dynamics to Study the Mixing of Pseudoplastic Fluids", M.A.Sc. Thesis, Ryerson University, Toronto (2007).
- Kelly W., Gigas, B., 2003. "Using CFD to predict the behavior of power law fluids near axial-flow impellers operating in the transitional flow regime", *Chem. Eng. Sci.*, 58, 2141-2152.
- Mishra V.P., Dyster K.N., Jaworski Z., Nienow A.W., Mckemmie J., 1998. "A study of an up- and a down-pumping wide blade hydrofoil impeller: Part I. LAD measurements", *Can. J. Chem. Eng.*, 76, 577-588.
- Ein-Mozaffari F., Dumont G.A., Bennington C.P.J., 2003. "Performance and design of agitated pulp stock chests", *Appita J.*, 56, 127-133.
- Houcine, I., Plasari E., David R., 2000. "Effects of the stirred tank's design on power consumption and mixing time in liquid phase", *Chem. Eng. Technol.*, 23, 605-613.
- Aubin J, Mavros P., Fletcher D.F., Bertrand J., Xuereb C., 2001. "Effect of axial agitator configuration (up-pumping, down-pumping, reverse-rotation) on flow patterns generated in stirred vessels", *Chem. Eng. Res. Des.*, 79, 845-856.